Searching for Fossil Fields in the Gravity Sector

Emanuela Dimastrogiovanni,[1] Matteo Fasiello,[2] and Gianmassimo Tasinato[3]
[1]School of Physics, The University of New South Wales, Sydney, New South Wales 2052, Australia
[2]Institute of Cosmology and Gravitation, University of Portsmouth, Portsmouth PO1 3FX, United Kingdom
[3]Department of Physics, Swansea University, Swansea SA2 8PP, United Kingdom

(Received 23 July 2019; revised manuscript received 5 November 2019; accepted 23 January 2020; published 12 February 2020)

Evidence for the presence of extra fields during inflation may be found in the anisotropies of the scalar and tensor spectra across a vast range of scales. Indeed, beyond the single-field slow-roll paradigm, a long tensor mode modulating the power spectrum can induce a sizable quadrupolar anisotropy. We investigate how these dynamics play out for the tensor two-point correlator. The resulting quadrupole stores information on squeezed tensor non-Gaussianities, including those sourced by extra field content and responsible for the breaking of so-called consistency relations. We underscore the potential of anisotropies as a probe of new physics: testable at cosmic microwave background scales through the detection of B modes, they are accessible at smaller scales via pulsar timing arrays and interferometers. Our findings are particularly relevant in that recent studies show a considerable suppression for tensor non-Gaussianities if all modes are well inside the horizon. Quadrupolar anisotropies instead probe an unsuppressed ultrasqueezed bispectrum where the long mode can be horizon size.

DOI: 10.1103/PhysRevLett.124.061302

Introduction.—The detection of gravitational waves from black hole mergers and from colliding neutron stars [1] has ushered in a new era for astronomy. The same is bound to happen for early Universe cosmology upon observing (evidence of) a primordial tensor signal. In particular, probes of the gravity sector hold great discovery potential when it comes to inflationary physics. Detection of cosmic microwave background (CMB) B-mode polarization would, in standard single-field slow-roll scenarios, precisely identify the energy scale of inflation. Crucially, gravitational probes can also access precious information on the early acceleration phase in the case of multifield inflation.

Nonminimal inflationary field content is not only possible but perhaps even likely [2]. String theory realizations of the acceleration mechanism typically result in extra dynamics. The additional field content acts as a source of the standard inflationary scalar and tensor fluctuations. An interesting phenomenology ensues whereby tensor fluctuations may deliver a nonstandard tensor power spectrum exhibiting a marked scale dependence, features, and, in specific cases [3–8], a chiral signal. Interestingly, a similar dynamics is arrived at by employing alternative (broken) symmetry patterns [9] or so-called nonattractor phases for the inflationary mechanism [10,11].

Perhaps the most sensitive probe of extra physics is the bispectrum. Remarkably, the soft momentum limit of the bispectrum contains detailed information [12] on the mass, the spin, and (implicitly) the couplings of extra fields. The existence of a nontrivial squeezed bispectrum contribution, mediated by the extra content, may be inferred already at the level of the tensor power spectrum. Indeed, in what we shall call the *ultrasqueezed* configuration, a long tensor mode induces a position dependence in the short mode power spectrum. In this context, a nontrivial bispectrum corresponds to one that modifies so-called consistency relations (CRs). These are maps between "soft" limits of $(N+1)$-point functions and their lower order counterpart that result from a residual diffeomorphism in the description of the physical system. Standard inflationary CRs are modified in the presence of, e.g., non-Bunch-Davies initial conditions, independent modes that transform nonlinearly under the diffeomorphism, alternative symmetry breaking patterns, etc., [13]. A prototypical example of modified CRs stems from the presence of extra fields during inflation. Interactions mediated by the extra σ content (see Fig. 1) are precisely those that can modify CRs.

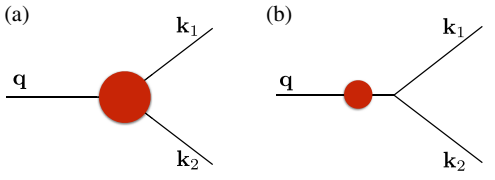

FIG. 1. Tensor three-point function mediated by extra σ fields. Red circles indicate interactions between metric tensor modes and σ fields. Diagrams leading to a consistency-relation-breaking bispectrum are the subset of those in (a) that cannot be simplified to the form in (b). Indeed, the latter diagram is sensitive to information on σ that is already accessible via the standard tensor two-point function.

As a result of the CRs breaking, the σ-mediated leading contribution to the squeezed bispectrum is physical and cannot be gauged away.

In what follows, we study the power spectrum of tensor fluctuations in the presence of a long-wavelength tensor mode. The resulting modulation can occur at widely different scales, from the CMB to regimes accessible via interferometers. In the quadrupolar anisotropy section, we analyze in detail how the squeezed tensor bispectrum [14] induces a quadrupolar anisotropy in the power spectrum. In the gravitational wave propagation and ultrasqueezed bispectrum section, building on recent important work [15,16], we elaborate on the fact that such observable is not plagued by the suppression effects that prevent a direct measurement of tensor non-Gaussianity at interferometer scales. We offer our conclusions in the final section.

Quadrupolar anisotropy.—If inflation predicts a nontrivial [17] tensor-scalar-scalar bispectrum in the squeezed limit (the tensor being the soft mode), a quadrupolar anisotropy is induced by the long-wavelength mode in the observed *local* scalar power spectrum [22]. In close analogy to the procedure developed for the scalar case, the tensor power spectrum is modulated by a long-wavelength tensor fluctuation. The quadrupolar anisotropy of the tensor power spectrum is then an observable sensitive to the squeezed limit of tensor non-Gaussianity.

The starting point is the correlation between two tensor modes in the presence of a long-wavelength mode [23]:

$$\langle \gamma^{\lambda_1}_{\mathbf{k}_1}\gamma^{\lambda_2}_{\mathbf{k}_2}\rangle_{\gamma_L} \equiv (2\pi)^3\delta^{\lambda_1\lambda_2}\delta^{(3)}(\mathbf{k}_1+\mathbf{k}_2)P^{\lambda_1}_{\gamma}(k_1)+\sum_{\lambda_3}\int_{|\vec{q}|<q_L} d^3q\,\delta^{(3)}(\mathbf{k}_1+\mathbf{k}_2+\mathbf{q})\gamma^{*\lambda_3}_{\mathbf{q}}\frac{B^{\lambda_1\lambda_2\lambda_3}_{\gamma}(\mathbf{k}_1,\mathbf{k}_2,\mathbf{q})}{P^{\lambda_3}_{\gamma}(q)}, \tag{1}$$

where q_L is a cutoff on whose size we shall soon elaborate. It suffices here to say that we ensure that we integrate only over the squeezed configurations of the bispectrum B_γ. $P^{\lambda_1}_{\gamma}(k)$ is the isotropic part of the tensor power spectrum, and we adopted the usual Fourier mode decomposition $\gamma_{\mathbf{k},ij}(\tau)=\sum_{\lambda=R,L}\epsilon^{\lambda}_{ij}(\mathbf{k})\gamma^{\lambda}_{\mathbf{k}}(\tau)$. Note that, in Eq. (1) and the rest of this section, we omit the time dependence of γ^{λ}_{k}. This is because for long modes, such as those corresponding to CMB observables, one can work in the $k\eta \ll 1$ limit where tensor fluctuations are frozen and purely primordial: $\gamma_k \simeq \gamma^{\rm prim}_k$. This is in contradistinction to Eq. (9) and the associated quantities in the following section: short modes propagating the horizon undergo time evolution.

The tensor bispectrum in Eq. (1) is given by

$$\langle \gamma^{\lambda_3}_{\mathbf{q}}\gamma^{\lambda_1}_{\mathbf{k}_1}\gamma^{\lambda_2}_{\mathbf{k}_2}\rangle \equiv (2\pi)^3\delta^{(3)}(\mathbf{k}_1+\mathbf{k}_2+\mathbf{q})B^{\lambda_1\lambda_2\lambda_3}_{\gamma}(\mathbf{k}_1,\mathbf{k}_2,\mathbf{q}).$$

In standard single-field models, the leading terms in B_γ are related to the scale dependence of the (short) tensor power spectrum through consistency relations [24]. As a result, their effect can be removed by an appropriate gauge transformation (see, e.g., Refs. [22,25–28]). In models where consistency relations are modified or broken, B_γ accesses directly new physical information stored in the squeezed tensor bispectrum. It is in the latter cases that our analysis becomes especially relevant. In what follows, it will be convenient to use the quantity $\tilde{B}$, defined as

$$B^{\lambda_1\lambda_2\lambda_3}_{\gamma}|_{q\ll k_{1,2}} \simeq -\delta^{\lambda_1\lambda_2}\epsilon^{\lambda_3}_{\ell m}(\hat{q})\hat{k}_{1\ell}\hat{k}_{2m}\tilde{B}(\mathbf{k}_1,\mathbf{k}_2,\mathbf{q}). \tag{2}$$

After a few algebraic manipulations, one finds the following expression for the tensor power spectrum in the presence of a long-wavelength tensor mode $\gamma_{\mathbf{q}}$, evaluated locally, i.e., within a volume whose linear dimension is smaller than the wavelength of the tensor ($|\mathbf{x}| \ll 1/q$):

$$\begin{aligned} P_\gamma(\mathbf{k},\mathbf{x}_c)|_{\gamma_L} &\equiv \int d^3x e^{-i\mathbf{k}\cdot\mathbf{x}}\left\langle \gamma_{ij}\left(\mathbf{x}_c-\frac{\mathbf{x}}{2}\right)\gamma_{ij}\left(\mathbf{x}_c+\frac{\mathbf{x}}{2}\right)\right\rangle_{\gamma_L} \\ &= P_\gamma(k)[1+\mathcal{Q}_{\ell m}(\mathbf{x}_c,\mathbf{k})\hat{k}_\ell\hat{k}_m]. \end{aligned} \tag{3}$$

The anisotropy is encoded in $\mathcal{Q}_{\ell m}$ as

$$\mathcal{Q}_{\ell m}(\mathbf{x}_c,\mathbf{k}) \equiv \int \frac{d^3q}{2\pi^3}e^{i\mathbf{q}\cdot\mathbf{x}_c}f^{\gamma}_{\rm nl}(\mathbf{q},\mathbf{k})\sum_{\lambda_3}\epsilon^{\lambda_3}_{\ell m}(-\hat{q})\gamma^{*\lambda_3}_{-\mathbf{q}}. \tag{4}$$

Note that in Eq. (4) the parametrization $\tilde{B}(\mathbf{k},\mathbf{q}) = f^{\gamma}_{\rm nl}(\mathbf{q},\mathbf{k})P_\gamma(k)P_\gamma(q)$ has been adopted, where $f^{\gamma}_{\rm nl}$ codifies the amplitude and momentum dependence of the squeezed limit of the tensor bispectrum. While the ensemble average $\bar{Q}$ vanishes, its variance does not, with it being derived from the tensor two-point function.

Expanding the quadrupole modulation in spherical harmonics and computing its variance, one arrives at

$$\begin{aligned} \overline{\mathcal{Q}^2} &\equiv \left\langle \sum_{m=-2}^{+2}|\mathcal{Q}_{2m}|^2\right\rangle \\ &= \frac{8\pi}{15}16\int\frac{d^2\hat{q}}{4\pi}\int_{q^{\rm min}}^{q^{\rm max}}\frac{dq}{q}(f^{\gamma}_{\rm nl})^2(\mathbf{q},\mathbf{k})\mathcal{P}_\gamma(q), \end{aligned} \tag{5}$$

where $\mathcal{P}_\gamma(q) \equiv q^3P_\gamma(q)/2\pi^2$. We pause here to comment on how the extrema of integration over q are chosen. The lower value $q^{\rm min}$ is selected as the wave number corresponding to the longest wavelengths that ever exited the horizon. The value of $q^{\rm max}$ depends instead on the specific probe. For CMB observations, for example, $q^{\rm max}$ is given

by the smallest wave number probed by a given experiment. The case of interferometers will be the subject of a more detailed discussion in the gravitational wave propagation section. As we shall see, in such a case the momentum $q_{\rm max}$ is limited to be, at most, horizon size. This corresponds to probing the ultrasqueezed bispectrum configuration.

Whenever $f^{\gamma}_{\rm nl}$ and the power spectrum $\mathcal{P}_\gamma$ are scale invariant, Eq. (5) simplifies to

$$\overline{\mathcal{Q}^2} = 8\pi \frac{16}{15} (f^{\gamma}_{\rm nl})^2 \mathcal{P}_\gamma \ln\left(\frac{q^{\rm max}}{q^{\rm min}}\right). \tag{6}$$

Models of (super)solid [29,30] and nonattractor [10] inflation do indeed support an (almost) scale-invariant profile for both the power spectrum and $f^{\gamma}_{\rm nl}$. Let us focus on Eq. (6) in the case of CMB polarization. Recalling the definition of the tensor-to-scalar ratio as $r \equiv \mathcal{P}_\gamma/\mathcal{P}_\zeta$, one finds that

$$\sqrt{\overline{\mathcal{Q}^2}} = 2.4 \times 10^{-4} f^{\gamma}_{\rm nl} \sqrt{r \Delta N}, \tag{7}$$

where the number of e-folds between the exit of the longest mode $q^{\rm min}$ and the exit of $q^{\rm max}$ is $\Delta N \equiv \ln(q^{\rm max}/q^{\rm min})$. As an example, with $\Delta N = O(1)$, a value for $\sqrt{\overline{\mathcal{Q}^2}}$ of order 0.1 requires $f^{\gamma}_{\rm nl}\sqrt{r} \simeq 500$. Given current constraints on the tensor-to-scalar ratio, this demands $f^{\gamma}_{\rm nl} \gtrsim 2 \times 10^3$. It would be interesting to forecast the bounds that future CMB polarization experiments will be able to place on squeezed non-Gaussianity by probing the tensor quadrupolar anisotropy. We leave this to future work.

If the tensor power spectrum or $f^{\gamma}_{\rm nl}$ is not scale invariant, the expression for the quadrupole anisotropy is modified with respect to Eq. (6). As a concrete example, let us consider a tensor bispectrum mediated by a massive spin-2 field [18,19]. In this setup, for a mass of the spin-2 field of order Hubble, the square root of the quadrupole variance is typically of order 10^{-1} on CMB scales. We note here that models with excited initial states (see, e.g., Ref. [31]) are also of interest for quadrupolar anisotropies: in some of these constructions, $f^{\gamma}_{\rm nl}$ scales with negative powers of q/k, which may easily lead to a sizable quadrupole.

Anisotropies at smaller scales:—If the primordial gravitational wave (GW) spectrum has a sufficiently large amplitude at small scales (see, e.g., Ref. [32]), anisotropies of the stochastic GW background can be accessed (see the following section) via both interferometers and pulsar timing arrays (PTAs).

The formalism for the analysis of anisotropies of stochastic gravitational wave backgrounds (SGWBs) with ground- and space-based detectors was introduced in Refs. [33,34]. Techniques developed for PTAs can be found in Refs. [35,36]. These studies are motivated by astrophysical phenomena: anisotropies can be associated with groups of unresolved sources on localized regions of the sky, such as large cosmic structures. Similar methods are applicable in the context of our Letter, where anisotropies have a primordial origin and $\mathcal{Q}_{ij}$ is characterized by random matrix entries obeying Gaussian statistics. We shall adopt the notation of the classic work [37]. The overlap function γ_{12}, associated with the cross-correlation of signals measured with a pair of ground-based detectors, receives contributions due to tensor anisotropies. In the vanishing frequency limit and small antenna regime, we find a simple analytic expression for the correction associated with the quadrupolar anisotropy described by Eq. (3):

$$\gamma_{12}(f \to 0) = 2 d_1^{ij} d_{2ij} - \frac{8}{7} \mathcal{Q}_{ij} (d_1^{im} d_{2m}^{j} + d_2^{im} d_{1m}^{j}). \tag{8}$$

Here $d_a^{ij} \equiv 1/2(\hat{X}_a^i \hat{X}_a^j - \hat{Y}_a^i \hat{Y}_a^j)$ denotes the detector tensor, and $\hat{X}_a$, $\hat{Y}_a$ the interferometer arm directions. At high frequencies, the contributions of the anisotropy to the overlap function are suppressed (see Fig. 2), and one recovers the results of Ref. [37]. Anisotropies of SGWBs can then be detected and analyzed through their distinctive effects on a daily modulation of the signal [33].

One might wonder how to distinguish primordial sources of quadrupolar anisotropy from astrophysical ones. A bispectrum with a large component in the squeezed configuration can induce anisotropies in the GW spectrum at both CMB and interferometer scales. If the signal is sufficiently broad to be measurable by two independent probes, one may search for common properties in the tensor quadrupolar harmonics, which would then hint at a

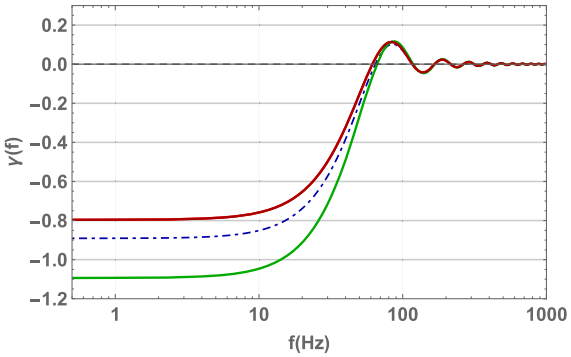

FIG. 2. The total overlap function $\gamma_{12}(f)$ for the cross-correlation of LIGO Hanford–LIGO Livingston detectors as a function of frequency, evaluated in the small antenna regime. We consider two examples of quadrupolar anisotropy in the SGWB. The blue dashed line indicates the standard result in the absence of anisotropy. The red line accounts for a quadrupolar anisotropic contribution with random matrix entries Q_{ij}. The green line is the same as the red line, except that the quadrupolar anisotropy is now associated with a specific direction n^i in the sky: $Q_{ij} = n_i n_j$. In both cases, the sum of the squares of the Q_{ij} eigenvalues is of order 0.35. Notice that the anisotropic contributions are relevant only at small frequencies.

primordial origin for the anisotropies. We leave such investigations for future work.

GW propagation and ultrasqueezed bispectrum.—We saw in the previous section how a long tensor mode can induce anisotropies in the power spectrum. At CMB scales, the quadrupole serves as an indirect probe of squeezed non-Gaussianity, complementary to direct measurements of three-point correlations of temperature and polarization anisotropies. Is the same possible at small scales? Two recent works [15,16] have shown that primordial tensor non-Gaussianity *cannot* be probed directly, i.e., by measuring three (or higher connected) point functions of tensor fluctuations at interferometer scales. Paraphrasing Ref. [15], measurements of primordial tensor modes correlations at small scales involve angular integrations of contributions from signals produced by a large number of separate, independent Hubble patches. In light of the central limit theorem, the statistics of tensor perturbations measured at interferometer scales will then be Gaussian. One would not be able to detect non-Gaussian correlations even in the case of a set of detectors built with the specific purpose of probing a large number of Hubble patches. Indeed, tensor non-Gaussianity at small scales is suppressed due to the Shapiro time delay associated with the propagation of tensor modes at subhorizon scales in the presence of matter. Reference [15] suggests that observables sensitive to large correlations between short- and long-wavelength tensor modes, induced, for example, by an ultrasqueezed bispectrum, may escape these conclusions. A concrete realization of such a possibility is precisely the quadrupolar anisotropy of the power spectrum discussed in the previous section, which relies in part on previous works for the scalar [20,38] and tensor [10,29,39] cases.

As we shall see in some detail below, the quadrupolar asymmetry survives the aforementioned suppression effects because it is induced by an (at least) *horizon-size* fluctuation.

Propagation at subhorizon scales:—We start by reviewing how propagation affects short-wavelength modes [16]. In doing so, we make sure to account for the subhorizon evolution of the short-wavelength tensor modes from horizon entry until detection at the interferometer. Their momenta being centered at interferometer frequencies, short modes have entered the horizon during the radiation-dominated era. The time evolution of such modes (and derived quantities such as the power spectrum and bispectrum) is a key qualitative difference that characterizes anisotropies at small vs large scales. For $k > k_{\rm eq}$ and $\eta < \eta_{\rm eq}$, with $\eta_{\rm eq}$ being the time of matter-radiation equality, the mode function reads

$$\gamma_{\mathbf{k}}^{\rm RD}(\eta) = j_0(k\eta)\gamma_{\mathbf{k}}^{\rm prim}, \tag{9}$$

where $j_0(k\eta) = \sin(k\eta)/(k\eta)$ is the spherical Bessel function, and $\gamma_{\mathbf{k}}^{\rm prim} = \gamma_k^{\rm prim} a_{\mathbf{k}} + \gamma_k^{\rm prim*} a_{-\mathbf{k}}^{\dagger}$ the primordial tensor perturbation. During matter domination, and to leading order in $|k\eta|$, one has [16,40]

$$\gamma_{\mathbf{k}}(\eta) \simeq \frac{1}{(k\eta)^2}[\mathcal{C}(\mathbf{k})e^{i\Gamma(\mathbf{k},\eta)} + \mathcal{C}^{\dagger}(-\mathbf{k})e^{-i\Gamma(-\mathbf{k},\eta)}], \tag{10}$$

where $\mathcal{C}(\mathbf{k})$ is a constant operator and

$$\begin{aligned}\Gamma(\mathbf{k},\eta) &= k\eta + 2k\int_{\eta_{\rm eq}}^{\eta} d\eta' \Phi(\eta', (\eta'-\eta_0)\hat{k}) \\ &\equiv k\eta + Z(\mathbf{k},\eta),\end{aligned} \tag{11}$$

with Φ being the Newtonian potential. The above expressions underscore that inhomogeneities in the matter density at small scales affect the evolution of tensor modes. Matching Eqs. (9) and (10) at the time of matter-radiation equality, the solution for $\eta > \eta_{\rm eq}$ becomes

$$\gamma_{\mathbf{k}}(\eta) = \frac{\eta_{\rm eq}}{k\eta^2}\left(\frac{e^{i\Gamma(\mathbf{k},\eta)} - e^{-i\Gamma(-\mathbf{k},\eta)}}{2i}\right)\gamma_{\mathbf{k}}^{\rm prim}. \tag{12}$$

We now consider the local power spectrum of gravitational waves evaluated in the presence of long-wavelength tensor perturbations, at a generic time η during matter domination:

$$\begin{aligned}\langle \gamma_{ij}^{\lambda_1}(\mathbf{k}_1,\eta)\gamma_{ij}^{\lambda_2}(\mathbf{k}_2,\eta)\rangle_{\gamma_L} = &\frac{\eta_{\rm eq}^2}{\eta^4 k_1 k_2}\frac{\epsilon_{ij}^{\lambda_1}(\hat{k}_1)\epsilon_{ij}^{\lambda_2}(\hat{k}_2)}{(-4)} \\ &\times \langle \gamma_{\mathbf{k}_1}^{\rm prim}\gamma_{\mathbf{k}_2}^{\rm prim}\rangle_{\gamma_L}\mathcal{E}(\mathbf{k}_1,\mathbf{k}_2,\eta).\end{aligned} \tag{13}$$

Here Eq. (12) has been used, $\langle \gamma_{\mathbf{k}_1}^{\rm prim}\gamma_{\mathbf{k}_2}^{\rm prim}\rangle_{\gamma_L}$ is given by Eq. (1), and

$$\mathcal{E} \equiv \langle (e^{i\Gamma(\mathbf{k}_1,\eta)} - e^{-i\Gamma(-\mathbf{k}_1,\eta)})(e^{i\Gamma(\mathbf{k}_2,\eta)} - e^{-i\Gamma(-\mathbf{k}_2,\eta)})\rangle. \tag{14}$$

The standard (isotropic) term on the first line of Eq. (1) produces the contribution

$$\begin{aligned}&\langle \gamma_{ij}^{\lambda_1}(\mathbf{k}_1,\eta)\gamma_{ij}^{\lambda_2}(\mathbf{k}_2,\eta)\rangle \\ &\quad = (2\pi)^3\delta^{\lambda_1\lambda_2}\delta^{(3)}(\mathbf{k}_1+\mathbf{k}_2)\frac{\eta_{\rm eq}^2}{2\eta^4 k_1^2}P^{\lambda_1}(k_1),\end{aligned} \tag{15}$$

where the expectation value in Eq. (14) was computed using the relation [16]

$$\langle e^{\varphi_1}e^{\varphi_2}\rangle = e^{(\langle\varphi_1^2\rangle/2)+(\langle\varphi_2^2\rangle/2)+\langle\varphi_1\varphi_2\rangle}. \tag{16}$$

The term in Eq. (1) proportional to the squeezed primordial bispectrum becomes instead

$$\langle \gamma_{ij}^{\lambda_1}(\mathbf{k}_1,\eta)\gamma_{ij}^{\lambda_2}(\mathbf{k}_2,\eta)\rangle_{\gamma_L} \supset -\frac{1}{4}\frac{\eta_{\rm eq}^2}{\eta^4 k_1 k_2}\epsilon_{ij}^{\lambda_1}(\hat{k}_1)\epsilon_{ij}^{\lambda_2}(\hat{k}_2)\times\sum_{\lambda_3}\int_{|\vec{q}|<q_L} d^3q\,\delta^{(3)}(\mathbf{k}_1+\mathbf{k}_2+\mathbf{q})\frac{\gamma_{\mathbf{q}}^{*\lambda_3}B_\gamma^{\lambda_1\lambda_2\lambda_3}(k_1,k_2,q)}{P_\gamma^{\lambda_3}(q)}\times\mathcal{E}(\mathbf{k}_1,\mathbf{k}_2,\eta). \tag{17}$$

Let us expand the expectation value on the last line of Eq. (17) using Eq. (11):

$$\begin{aligned}\mathcal{E}(\mathbf{k}_1,\mathbf{k}_2) = \langle & e^{i(k_1+k_2)\eta}e^{iZ(\mathbf{k}_1,\eta)}e^{iZ(\mathbf{k}_2,\eta)} \\ & + e^{-i(k_1+k_2)\eta}e^{-iZ(-\mathbf{k}_1,\eta)}e^{-iZ(-\mathbf{k}_2,\eta)} \\ & + e^{-i(k_1-k_2)\eta}e^{-iZ(-\mathbf{k}_1,\eta)}e^{iZ(\mathbf{k}_2,\eta)} \\ & + e^{i(k_1-k_2)\eta}e^{iZ(\mathbf{k}_1,\eta)}e^{-iZ(-\mathbf{k}_2,\eta)}\rangle. \end{aligned} \tag{18}$$

We anticipate here that, upon performing the momentum integration in Eq. (19), the contributions proportional to $e^{\pm i(k_1+k_2)\eta}$ [the first two lines of Eq. (18)] will vanish because of the highly oscillatory behavior. On the other hand, the relation between the wave numbers is $\mathbf{k}_1=-\mathbf{k}_2-\mathbf{q}$, with $k_1\simeq k_2\gg q$. The difference k_1-k_2 is therefore of the order of the inverse cosmic time, $1/\eta_0$ (with q being, at most, horizon size), and the exponentials $e^{\pm i(k_1-k_2)\eta}$ can be treated as constants when performing the momentum integrals. Moreover, in the ultrasqueezed configuration ($\mathbf{k}_1\simeq-\mathbf{k}_2$), the arguments of the Z terms on the last two lines in Eq. (18) are approximately equal, and one arrives at the (unsuppressed) $\mathcal{E}(\mathbf{k}_1,\mathbf{k}_2)\simeq-2$. It follows that the quadrupolar anisotropy of the tensor spectrum is not suppressed by propagation effects.

Averaging:—As noted in Ref. [15], the contributions of a primordial bispectrum to the three-point function of the detector time delay $\Delta\eta(\eta)$, as measured along the interferometer arms, vanishes as a result of rapidly oscillating phases $e^{i\sum_i\pm k_i\eta}$. This is not the case for the power spectrum: by enforcing $k_1=k_2$, the rapidly oscillating coefficient drops out. Let us now include the contribution due to coupling with long-wavelength tensor fluctuations to the time delay two-point function. We find

$$\begin{aligned}\langle\Delta\eta(\eta)\Delta\eta(\eta)\rangle \sim \int & d^3k_1 d^3k_2 e^{i(\mathbf{x}_1\cdot\mathbf{k}_1+\mathbf{x}_2\cdot\mathbf{k}_2)}e^{i(k_1-k_2)\eta} \\ & \times\mathcal{M}(\hat{L}_1\cdot\hat{k}_1,k_1)\mathcal{M}^*(-\hat{L}_2\cdot\hat{k}_2,k_2) \\ & \times\langle\gamma(\mathbf{k}_1,\eta)\gamma(\mathbf{k}_2,\eta)\rangle_{\gamma_L}, \end{aligned} \tag{19}$$

with $\mathcal{M}$ being the detector transfer function, and $\hat{L}_i$ the interferometer arm direction. The expectation value on the last line of Eq. (19) now also includes the off-diagonal term proportional to the primordial bispectrum. The actual observable consists of the Fourier transform of Eq. (19). As a result, a factor of $e^{i(k_1-k_2)\eta_0}$ will emerge. The long-wavelength mode q being at least horizon size, one has $|k_1-k_2|\simeq q$, with $q\leq\eta_0^{-1}$, where η_0 is the cosmic time. It follows that $|k_1-k_2|\eta_0\simeq q\eta_0\leq 1$ and, as with the isotropic power spectrum, no suppression occurs. The part controlled by the squeezed bispectrum selectively picks up the contribution of signals emitted from the same Hubble patch. The Fourier transform of Eq. (19) leads to an observable proportional to the observation time T. Depending on the strength of the long-short mode coupling codified in the primordial bispectrum $\mathcal{B}_\gamma^{\lambda_1\lambda_2\lambda_3}$, a larger (smaller) observation time will be required for detection.

We conclude that the quadrupole anisotropy computed in the quadrupolar anisotropy section propagates all the way to the observed GW power spectrum.

Conclusions.—The observables that hold the most promise to access key information on inflationary dynamics are the power spectrum and the bispectrum of primordial correlation functions, in both the scalar and tensor sectors. The corresponding predictions for the minimal inflationary scenario have long been known. Any observed deviation would therefore point directly to new physics. Unknowns still characterize the tensor sector where the predicted primordial signal remains undetected. The advent of ground- and space-based interferometers makes it possible to test for inflationary models with a nonstandard scale dependence in the tensor spectrum and search for telltale signs of their particle content.

Recent studies [15,16] have shown that the primordial tensor bispectrum is strongly suppressed at interferometer scales. Among other effects, propagation through structure decorrelates primordial modes of different wavelengths. Accessing the bispectrum directly at interferometer (or, e.g., PTA) scales necessarily implies that all of the modes have undergone subhorizon evolution. In this Letter, we have put forward a complementary approach: looking for quadrupolar anisotropies in the tensor power spectrum as a probe of the primordial tensor bispectrum. The quadrupole is sensitive to modulations of a horizon-size tensor mode on the GW power spectrum. In this configuration, one mode is insensitive to propagation, while the remaining two are very similar, thereby avoiding a strong suppression. Quadrupolar tensor anisotropies can therefore be probed at widely different frequency ranges and represent an efficient tool for testing inflationary models that support an ultrasqueezed component of the tensor bispectrum.

We are delighted to thank Valerie Domcke and Toni Riotto for their comments on the manuscript, and David Wands for discussions on the subject. G. T. would also like

to thank Nicola Bartolo, Ogan Özsoy, Marco Peloso, Angelo Ricciardone, and Toni Riotto for the discussions. The work of M. F. is supported in part by UK STFC Grant No. ST/S000550/1. The work of G. T. is partially supported by STFC Grant No. ST/P00055X/1.

[1] B. P. Abbott *et al.* (LIGO Scientific and Virgo Collaborations), Phys. Rev. Lett. **116**, 061102 (2016); **119**, 161101 (2017).
[2] D. Baumann and L. McAllister, *Inflation and String Theory*, Cambridge Monographs on Mathematical Physics (Cambridge University Press, Cambridge, England, 2015).
[3] M. M. Anber and L. Sorbo, Phys. Rev. D **81**, 043534 (2010).
[4] N. Barnaby and M. Peloso, Phys. Rev. Lett. **106**, 181301 (2011).
[5] P. Adshead and M. Wyman, Phys. Rev. Lett. **108**, 261302 (2012).
[6] E. Dimastrogiovanni, M. Fasiello, and T. Fujita, J. Cosmol. Astropart. Phys. 01 (2017) 019.
[7] E. Pajer and M. Peloso, Classical Quantum Gravity **30**, 214002 (2013).
[8] J. Garcia-Bellido, M. Peloso, and C. Unal, J. Cosmol. Astropart. Phys. 12 (2016) 031.
[9] S. Endlich, A. Nicolis, and J. Wang, J. Cosmol. Astropart. Phys. 10 (2013) 011.
[10] O. Ozsoy, M. Mylova, S. Parameswaran, C. Powell, G. Tasinato, and I. Zavala, J. Cosmol. Astropart. Phys. 09 (2019) 036.
[11] M. Mylova, O. Ozsoy, S. Parameswaran, G. Tasinato, and I. Zavala, J. Cosmol. Astropart. Phys. 12 (2018) 024.
[12] N. Arkani-Hamed and J. Maldacena, arXiv:1503.08043.
[13] K. Hinterbichler, L. Hui, and J. Khoury, J. Cosmol. Astropart. Phys. 01 (2014) 039.
[14] See, e.g., Sec. V of N. Bartolo, V. Domcke, D. G. Figueroa, J. Garcia-Bellido, M. Peloso, M. Pieroni, A. Ricciardone, M. Sakellariadou, L. Sorbo, and G. Tasinato, J. Cosmol. Astropart. Phys. 11 (2018) 034 for a review on tensor non-Gaussianity from inflation.
[15] N. Bartolo, V. De Luca, G. Franciolini, A. Lewis, M. Peloso, and A. Riotto, Phys. Rev. Lett. **122**, 211301 (2019).
[16] N. Bartolo, V. De Luca, G. Franciolini, M. Peloso, D. Racco, and A. Riotto, Phys. Rev. D **99**, 103521 (2019).
[17] We refer the reader interested in explicit models to the work in Refs. [18–21] and the references therein. See also Fig. 1(a) for a diagrammatic representation.
[18] L. Bordin, P. Creminelli, A. Khmelnitsky, and L. Senatore, J. Cosmol. Astropart. Phys. 10 (2018) 013.
[19] E. Dimastrogiovanni, M. Fasiello, G. Tasinato, and D. Wands, J. Cosmol. Astropart. Phys. 02 (2019) 008.
[20] E. Dimastrogiovanni, M. Fasiello, and M. Kamionkowski, J. Cosmol. Astropart. Phys. 02 (2016) 017.
[21] R. Emami and H. Firouzjahi, J. Cosmol. Astropart. Phys. 10 (2015) 043.
[22] L. Dai, D. Jeong, and M. Kamionkowski, Phys. Rev. D **88**, 043507 (2013).
[23] D. Jeong and M. Kamionkowski, Phys. Rev. Lett. **108**, 251301 (2012).
[24] J. M. Maldacena, J. High Energy Phys. 05 (2003) 013.
[25] M. Gerstenlauer, A. Hebecker, and G. Tasinato, J. Cosmol. Astropart. Phys. 06 (2011) 021.
[26] S. B. Giddings and M. S. Sloth, Phys. Rev. D **84**, 063528 (2011).
[27] L. Dai, E. Pajer, and F. Schmidt, J. Cosmol. Astropart. Phys. 11 (2015) 043.
[28] V. Sreenath and L. Sriramkumar, J. Cosmol. Astropart. Phys. 10 (2014) 021.
[29] A. Ricciardone and G. Tasinato, J. Cosmol. Astropart. Phys. 02 (2018) 011.
[30] A. Ricciardone and G. Tasinato, Phys. Rev. D **96**, 023508 (2017).
[31] S. Brahma, E. Nelson, and S. Shandera, Phys. Rev. D **89**, 023507 (2014).
[32] N. Bartolo *et al.*, J. Cosmol. Astropart. Phys. 12 (2016) 026.
[33] B. Allen and A. C. Ottewill, Phys. Rev. D **56**, 545 (1997).
[34] N. J. Cornish, Classical Quantum Gravity **19**, 1279 (2002).
[35] C. M. F. Mingarelli, T. Sidery, I. Mandel, and A. Vecchio, Phys. Rev. D **88**, 062005 (2013).
[36] S. C. Hotinli, M. Kamionkowski, and A. H. Jaffe, arXiv:1904.05348
[37] B. Allen and J. D. Romano, Phys. Rev. D **59**, 102001 (1999).
[38] E. Dimastrogiovanni, M. Fasiello, D. Jeong, and M. Kamionkowski, J. Cosmol. Astropart. Phys. 12 (2014) 050.
[39] E. Dimastrogiovanni, M. Fasiello, and G. Tasinato, J. Cosmol. Astropart. Phys. 08 (2018) 016.
[40] The formula below quantifies the Shapiro time delay. It is obtained by modeling the presence of matter via interactions between γ and ζ and working in the geometrical optic approximation.